applied sciences

MDPI

Article

Intelligent Control of the Microclimate of an Agricultural Greenhouse Powered by a Supporting PV System

Jamel Riahi [1], Silvano Vergura [2,*], Dhafer Mezghani [1] and Abdelkader Mami [1]

[1] UR-LAPER, Faculty of Sciences of Tunis, University of Tunis El Manar, 1068 Tunis, Tunisia; riahijamel100@gmail.com (J.R.); dhafer.mezghanni@gmail.com (D.M.); abdelkader.mami@fst.utm.tn (A.M.)

[2] Department of Electrical and Information Engineering, Polytechnic University of Bari, st. E. Orabona 4, I-70125 Bari, Italy

* Correspondence: silvano.vergura@poliba.it; Tel.: +39-080-596-3590

Received: 13 January 2020; Accepted: 13 February 2020; Published: 17 February 2020

Abstract: An agricultural greenhouse is a complex and Multi-Input Multi-Output MIMO system in which the internal parameters create a favorable microclimate for agricultural production. Temperature and internal humidity are two parameters that have a major impact on greenhouse yield. The objective of this study was to propose a simulated dynamic model in a MATLAB/Simulink environment for experimental validation. Moreover, a fuzzy controller was designed to manage a greenhouse indoor climate by means of an asynchronous motor for ventilation, heating, humidification, etc. An intelligent system to control these actuators for an optimal inside climate was implemented in the model. The dynamic model was validated by comparing the simulation results to experimental measurements. These results showed the effectiveness of the control strategy in regulating the greenhouse indoor climate. Finally, a photovoltaic generator was modeled, with the aim of reducing the costs of agricultural production. It feeds the asynchronous motor with a vector control optimized by fuzzy logic that drives a variable speed fan.

Keywords: dynamic model; fuzzy controller; photovoltaic generator; MPPT; converter SEPIC; vector control; MATLAB/Simulink environment

1. Introduction

Due to the enormous increase and instability of oil and derivatives markets, countries are constantly looking for alternative sources of energy to ensure the independence of their economies from fluctuations in oil prices. Photovoltaic energy can have undeniable advantages, especially due to its cleanliness and low cost. In addition, it can be used in various applications such as in agronomy, where different variables, e.g., temperature and humidity, have to be monitored and controlled. These include temperature and humidity. A greenhouse is a known solution for protecting plant cover from diseases and bad weather. A greenhouse is a complex system, the internal climate of which is influenced by many factors, such as wind speed, solar radiation, external temperature, and humidity. Two main problems have limited the expansion of greenhouse agricultural production.

Firstly, control over the indoor climate is an important aspect in achieving microclimate comfort for plant growth. Many research activities have focused on controlling the indoor climate of a greenhouse with different strategies. Predictive neural control [1] has been developed to optimize the greenhouse climate, while a fuzzy controller that was developed to describe a dynamic model in MATLAB/Simulink was described in Reference [2]. In addition, Reference [3] studied several PI control structures that showed strong stationary performance. In Reference [4], the authors introduced a decentralized decoupled fuzzy logic controller (FLC), showing its usefulness in comparison to the conventional PID

method, but they did not take into account the effect of ventilation on temperature. References [5,6] proposed a neuro-fuzzy controller to identify the optimal conditions for plant production and to improve control over the indoor climate. Genetic algorithms implemented in a control system for irrigation in a greenhouse were proposed in References [7,8], while Reference [9] presented a comparative study of two types of fuzzy multivariate controllers to show their advantages and disadvantages. Reference [10] developed four control techniques to adjust the air temperature inside a greenhouse to a desired value: fuzzy logic control (FLC), an adaptive neuro-fuzzy inference system (ANFIS), artificial neural network control (ANNC), and IP Control. ANFIS [11] and FLC [12] are two of the best known and most used controllers for nonlinear and complex processes such as greenhouses. Reference [13] presented a fuzzy controller with a correlation between the parameters. An FLC was used, in this paper, for the dynamic model of an experimentally validated agricultural greenhouse, with the aim of promoting a suitable microclimate with appropriate actuators installed into the greenhouse.

Secondly, the use of several controlled actuators, such as a ventilation system, a heating system, and a humidification/dehumidification system, makes a greenhouse an energy-intensive consumer. Therefore, it is mandatory to use efficient energy systems in order to reduce operating costs. Many researchers have studied control strategies for ventilation and heating systems, for humidification/dehumidification systems, and for the regulation of other agricultural greenhouse parameters. References [14,15] proposed a ventilation system based on an on–off control, Reference [16] studied a natural ventilation system for an agricultural greenhouse, Reference [17] presented an evaluation of the use of various renewable energy sources to heat a greenhouse, and Reference [18] introduced different fields of application for renewable energy in buildings, in particular in the agricultural sector. Reference [19] proposed energy reduction measured through low-cost and solar energy-based sensors. Reference [20] used direct torque control (DTC) to manage the operation of a motor driving a fan, while [21] discussed the application of a photovoltaic (PV) system to power a temperature control system in an agricultural greenhouse. These researchers were interested in the thermodynamic modeling of an agricultural greenhouse. Our paper combines the efficiency and robustness of control over the microclimate inside an agricultural greenhouse with optimization of the control strategy of a PV system that powers the internal actuators.

The contribution in the present work is the development and optimization of a ventilation system for a small greenhouse devoted to agricultural production. Energy consumption is reduced by coupling a PV system to an agricultural greenhouse. This approach provides a good solution to eliminating the overloading of an electricity grid. Moreover, the efficiency of the actual PV modules is good enough and can be easily monitored [22,23] if the PV system is equipped with a datalogger that stores the electrical parameters. Otherwise, in the absence of a datalogger, the correct operation of the PV systems can be checked by a thermo-camera [24,25] with the support of software that processes the infrared images [26,27]. The PV system plays the role of an energy source to power an asynchronous motor and to drive a fan controlled by vector control, which is optimized using a fuzzy logic strategy.

This paper has two parts. The first one (Sections 2–4) discusses the dynamic model of a greenhouse and the FLC. In particular, the dynamic model is presented in Section 2, and it was experimentally validated. The FLC, developed in Section 3, manages the inside temperature and humidity to control a variable speed ventilation system. The simulation results of the dynamic model are discussed in Section 4. The second part of the paper (Section 5) discusses the PV system and the operation of the powered electrical devices. Conclusions end the paper.

2. Dynamic Greenhouse Model

2.1. Greenhouse Model

A greenhouse is a system that can favor the growth of plants, because it guarantees suitable microclimate conditions for fixed cultivation. In fact, a greenhouse is a heat storing system that converts incident solar radiation into heat gain. This physical process is based on conduction, heat

storage, and convection. Control over the internal microclimate can be automatized (for example, by using a fuzzy controller, as in this paper) only if a physical model of the greenhouse is available. This model must be able to foresee changes in the indoor environmental parameters, which are based on several boundary conditions. For this reason, this section proposes—and validates experimentally—a simplified thermal model of a test lab greenhouse. The proposed model of the greenhouse is based on four layers (Figure 1) that participate in thermodynamic exchanges: the cover, the internal air, the plants, and the soil. The role of each layer is as follows:

- The main function of the cover is heat retention; usually, the cover is made of polyethylene film or glass;
- The interior air represents an internal climate that is mainly governed by temperature and humidity;
- The plants play a strategic role in water and heat balance, thanks to the evapotranspiration process [10];
- The soil influences the absorbance and diffusivity of the thermal radiation [11].

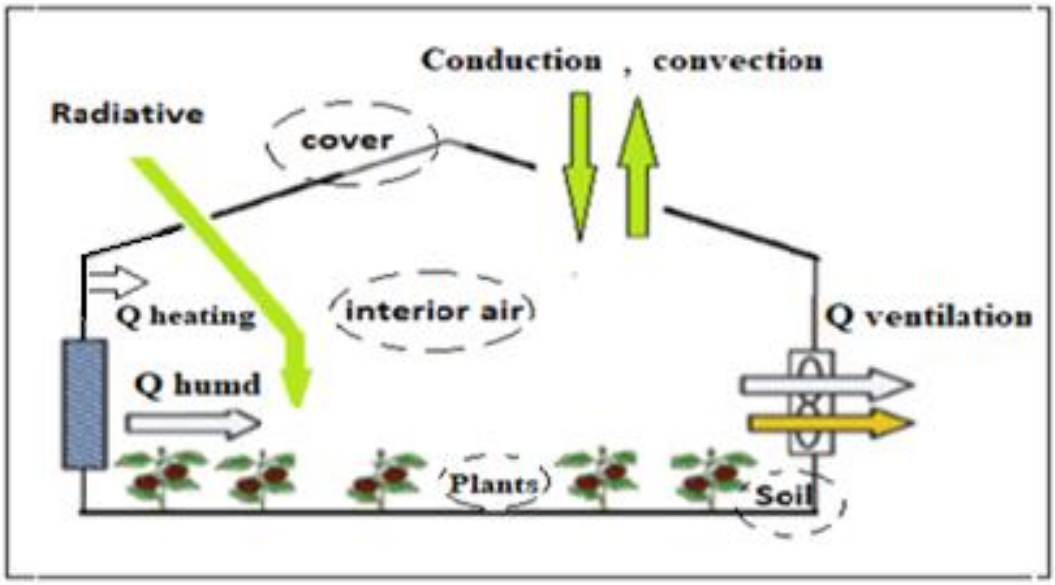

Figure 1. Schemes of greenhouse components.

2.2. Test Lab Greenhouse under Study

The greenhouse under investigation is in the north of Tunisia in the Borj Cedria region (36°43′10.25″ N) and is a typical model for greenhouses located in the Mediterranean area.

The greenhouse is a small, semi-insulated capel and occupies an area equal to 14.8 m^2 (width 3.7 m, length 4 m, ridge height 3 m), with a volume of 36 m^3. Therefore, it is a test lab greenhouse. Its shape, dimensions, and measuring equipment are presented in Reference [28]. The specific design of the semi-insulated greenhouse maximizes the contribution of solar radiation and reduces the loss of heat to the ground. The structure has a 0.4-m-thick panel on the side walls and on the ground. To prevent heat exchange between the soil and the climate inside the greenhouse, a wooden plate with a thermal conductivity $C_t = 0.04 \left(\mathrm{Wm^{-1}K^{-1}}\right)$ is used. Therefore, simplified modeling of the test lab greenhouse neglects heat transfer to the ground. Figures 2–4 show pictures of the greenhouse under investigation.

Figure 2. Experimental greenhouse.

Figure 3. HMP155A sensor.

Figure 4. Data acquisition unit.

2.3. Heat Balance

The air exchanges between the internal air and the external environment produce losses that affect the heat and water balance. The internal heat balance is governed by Equation (1) [2,13]:

$$\rho_a C_a v \frac{dtin}{dt} = Q^{short} + Q^{conv,cond} + Q^{infiltration} - Q^{long} + Q^{heater} - Q^{ventilation}, \quad (1)$$

where ρ_a is the air density [1.25 Kg·m^{-3}], and C_a is the air heat capacity (1003 J·Kg^{-1}·°C^{-1}).

The shortwave radiation absorbed by the greenhouse is given by

$$Q^{short} = \alpha_c \tau_c A I, \quad (2)$$

where α_c is the cover absorptivity of the solar radiation, τ_c is the cover transmittance, A is the surface area (m^2), and I is the solar radiation (Wm^{-2}).

The rate of convection and conduction heat transfer is calculated as

$$Q^{conv,cond} = UA(T_{in} - T_{out}), \quad (3)$$

where T_{in} is the internal temperature, T_{out} is the outside temperature (K), and U is the heat transfer coefficient through the greenhouse walls ($W \cdot m^{-2} \cdot K^{-1}$).

Infiltration through the greenhouse produces heat loss, which is calculated as

$$Q^{infiltration} = \rho_a C_a R \frac{T_{in} - T_{out}}{3600}, \quad (4)$$

where R is the number of air changes per hour ($m^3 \cdot h^{-1}$).

The longwave radiation absorbed by the greenhouse is calculated as

$$Q^{long} = h_o A (1 - \Gamma_c)\left(T_{in} - T_{sky}\right), \quad (5)$$

where

$$h_0 = 2.8 + (1.2 * V_w), \quad (6)$$

with V_w being the wind speed and T_{sky} being the sky temperature (as suggested by Swinbank in Reference [29]), which is calculated as

$$T_{sky} = 0,05(T_{out})^{1,5}. \quad (7)$$

The heating system provides thermal energy, which is calculated as

$$Q^{heater} = \frac{N_h R_h}{S}, \quad (8)$$

with N_h being the number of heaters, and R_h being the capacity of the heating system (Wm^{-2}).

The thermal energy lost from the cooling system is calculated as

$$Q^{ventilation} = C_a V_r (T_{in} - T_{out}), \quad (9)$$

where V_r is the ventilation rate ($m^3 s^{-1}$).

2.4. Water Balance

After the heat balance, the dynamics of the relative humidity inside the greenhouse need to be modeled. This is based on the following equation [2–22]:

$$\rho_a \, v \frac{dh_{in}}{dt} = Q^{evapotranspiration} - Q^{infiltration} + Q^{hum} - Q^{dehum}, \quad (10)$$

where h_{in} is the inside dynamic humidity calculated over time by a differential equation, while

$$Q^{evapotranspiration} = V C_e V_w (p_{out} - p_{in}), \quad (11)$$

where p_{in} and p_{out} are the inside and outside saturated vapor pressure (Pa), respectively; V is the volume of the greenhouse; V_w is the wind speed; and C_e is the transfer coefficient of the water vapor in the air (Kg. $(Wm^{-2}).s^{-1}.Pa^{-1}$).

$Q^{infiltration}$ inside the greenhouse is calculated as

$$Q^{\inf} = V_r (H_{in} - H_{out}), \quad (12)$$

where H_{in} and H_{out} are the inside and outside relative humidity, respectively.

2.5. Validation of the Proposed Dynamic Model

The proposed system was validated in a MATLAB/Simulink environment using a weather database of real measurements. This included measurements of solar radiation, wind speed, temperature, and

relative humidity. This also contained thermal properties of the greenhouse's response to external solar radiation. Some details are reported in Section 4.

The results of the theoretical simulations of the temperature and humidity were compared to the experimental measurements and are reported in Figures 5–7.

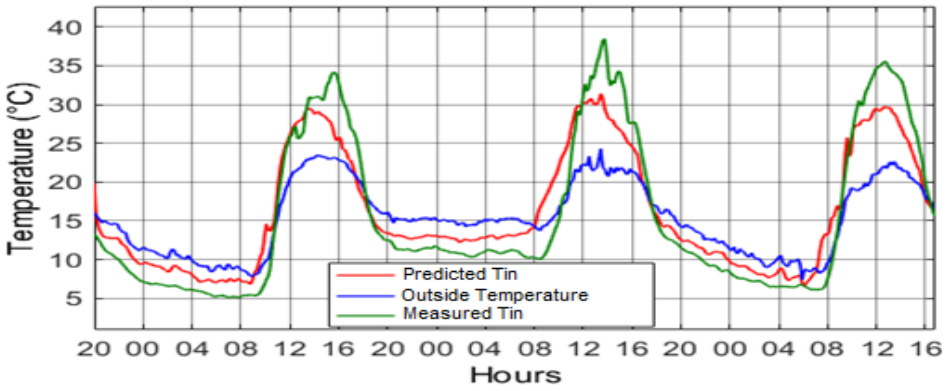

Figure 5. Measured and simulated data of the temperature inside the greenhouse.

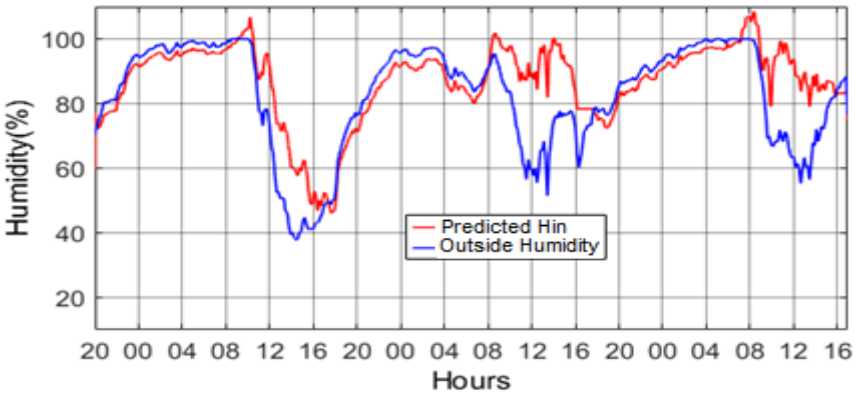

Figure 6. Simulation results of the inside and outside greenhouse humidity.

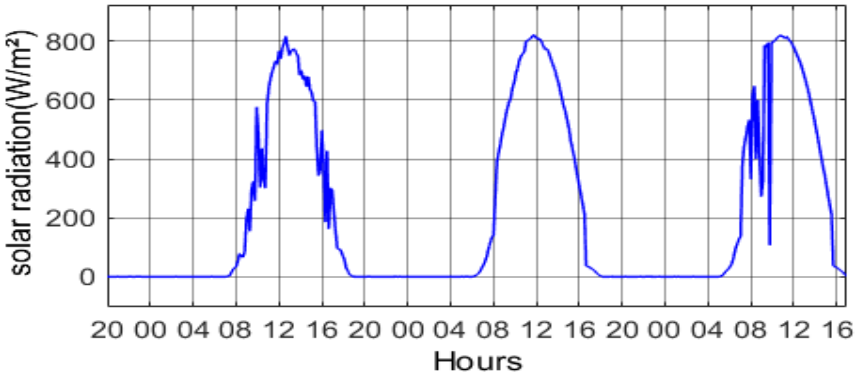

Figure 7. Real solar radiation.

Figure 5 shows a simulation of the greenhouse temperature over three days: the measured temperature (green curve) was measured by a sensor (Figure 3), the interior temperature (red curve) was calculated by a differential equation (Equation (1)), and the outside temperature (blue curve) was measured by a sensor outside the greenhouse.

The indoor and outdoor humidity are reported in Figure 6: the internal humidity (red curve) was calculated by a differential equation (Equation (10)), and the external humidity was measured by a sensor.

Figure 7 presents a database measuring solar radiation during the investigated period. The solar radiation data were measured using a sensor placed outside the greenhouse. The northern region of Tunisia is usually cold, so radiation is not particularly high. In fact, the authors in Reference [28] did the same measurements in that region (in another period), obtaining a maximum value of 700 W/m^2.

3. Fuzzy Logic Controller for the Greenhouse

The studied system is described in Figure 8.

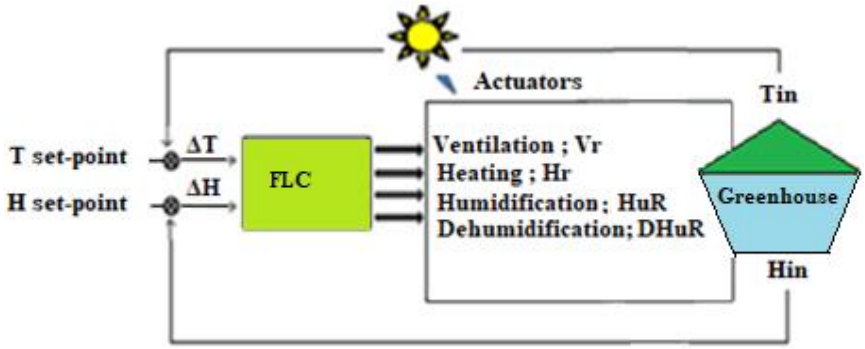

Figure 8. Schematic of the studied system.

The operation of the FLC is as follows: a comparison between the temperature (*Tin*) and the humidity (*Hin*) (with their set points) gives the errors ΔT and ΔH for the regulation of the internal factors of the greenhouse controlled by the actuators (ventilation, heating, etc.). In the next section, the architecture and design of the fuzzy controller are discussed.

When the actuators are active, the heat flow supplied by the heating system and the air flow of the ventilation system will be part of the thermodynamic model. Therefore, the temperature and the humidity inside the greenhouse are governed by Equations (1) and (10), respectively.

3.1. Architecture of the Fuzzy Control Unit

The fuzzy controller is based on a fuzzy inference engine (FIS), which consists of three main processing subsystems (Figure 9):

- A fuzzification interface that converts linguistics input variables into numerical values;
- A database unit that includes membership functions that need an "interface engine" in the fuzzy rules; and
- A defuzzification processor that generates crisp control output for specific actuators.

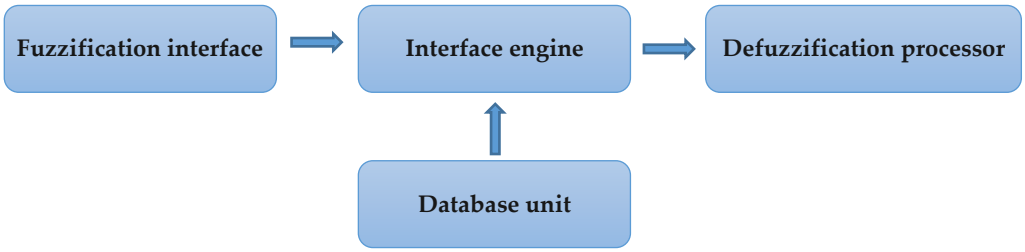

Figure 9. Fuzzy logic controller (FLC) architecture.

3.2. Temperature Control

The input state variable of the temperature fuzzy controller is ΔT (see Figure 8), where

$$\Delta T = Tsetpoint - Tin \in (NB, NM, Z, PM, PB). \quad (13)$$

The membership functions of the input temperature error are reported in Figure 10, where NB is negative big, NM is negative medium, Z is zero, PM is positive medium, and PB is positive big.

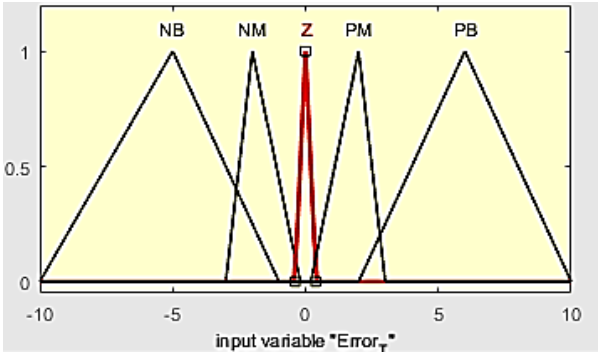

Figure 10. Membership functions of the temperature error.

The output variables are the ventilation rate (*Vr*) and the heating rate (*Hr*), with *Vr* ϵ (Z, M, H) and *Hr* ϵ (Z, M, H) (Z = zero, M = medium, and H = high).

Figure 11 reports the membership functions of the output variables, *Vr* and *Hr*.

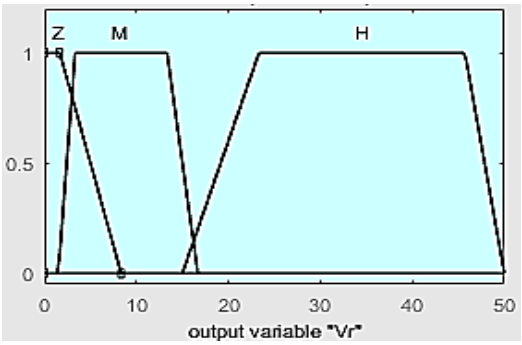

(**a**)

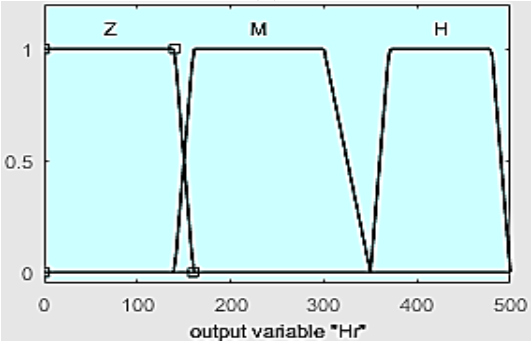

(**b**)

Figure 11. Membership functions of the output variables: (**a**) the ventilation rate *Vr* (**b**) and the heating rate *Hr*.

The membership function of the outputs is calculated as the maximum value of *Vr* = 50 m^3/min and *Hr* = 500 W/m^2.

3.3. Relative Humidity Control

The input state variable of the humidity fuzzy controller is Δ*H* in Figure 8, where

$$\Delta H = \text{Hsetpoint} - \text{Hin} \in (\text{NB, NM, Z, PM, PB}). \quad (14)$$

Figure 12 reports the membership functions of the input humidity error.

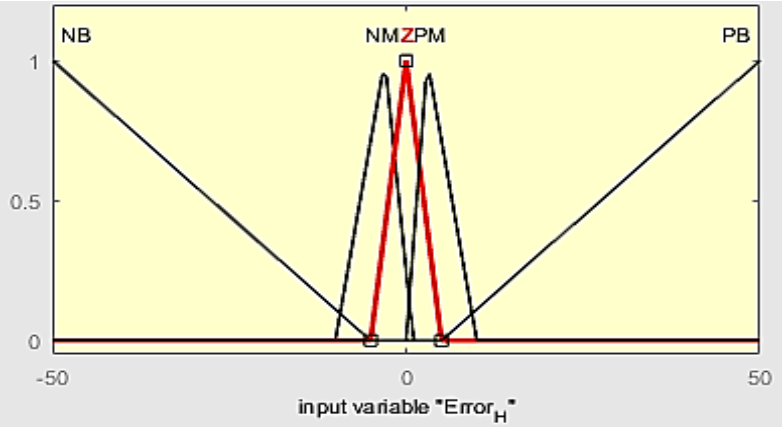

Figure 12. Membership functions of the humidity error.

The output variables are the humidification rate (*HuR*) and the dehumidification rate (*DHuR*), with (*HuR* and *DHuR*) ϵ (Z, M, H) (Z = zero, M = medium, and H = high).

The membership functions of the output variables are shown in Figure 13.

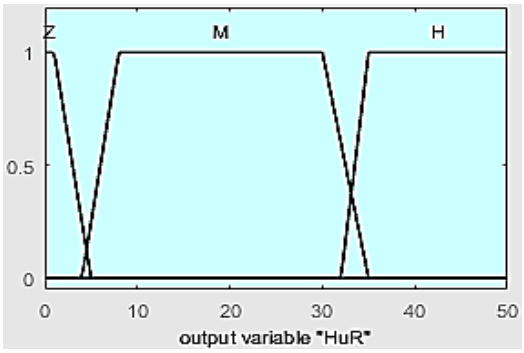

(**a**)

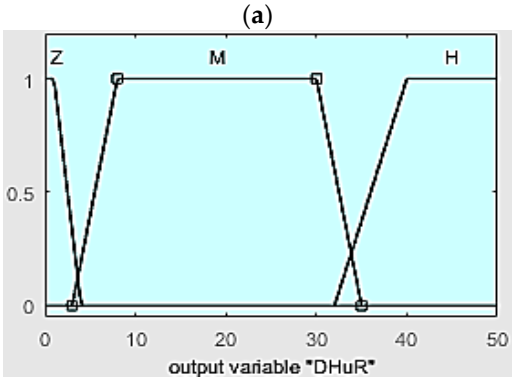

(**b**)

Figure 13. Membership functions of the output variables: (**a**) the humidification rate HuR (**b**) and the dehumidification rate DHuR.

The membership functions of the outputs *HuR* and *DHuR* are calculated in terms of a maximum value = 50 g_{H2O}/min.

Tables 1 and 2 present a basis for the fuzzy rules for temperature and humidity control. The bold rows highlight two examples that are useful in explaining the strategy:

- If (ΔT is negative big) then (ventilation is high) and (heating is zero); and
- If (ΔH is zero) then (humidification is zero) and (dehumidification is zero).

Table 1. Fuzzy rules for temperature control.

Temperature Error	Ventilation Rate	Heating Rate
Negative big	**High**	**Zero**
Negative medium	Medium	Zero
Zero	Zero	Zero
Positive medium	Zero	Medium
Positive big	Zero	High

Table 2. Fuzzy rules for the humidity controller.

Humidity Error	Humidification Rate	Dehumidification Rate
Negative big	Zero	High
Negative medium	Zero	Medium
Zero	**Zero**	**Zero**
Positive medium	Medium	Zero
Positive big	High	Zero

4. Simulations and Results

The simulation results of the fuzzy-controlled agricultural greenhouse are presented in Figure 14. Two different set points were set for the inside temperature: 15 °C for the night and 24 °C during the day. These reference values were fixed to guarantee optimal thermal conditions for cultivation (for tomato plants) in this test lab. Other reference values could be fixed for other cultivations. The same test for the inside humidity set two reference points: 70% during the day, and 80% during the night.

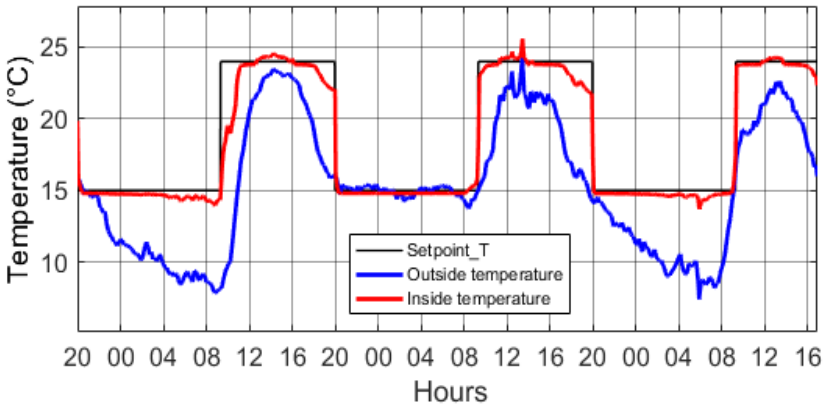

Figure 14. Simulation results for greenhouse temperature under fuzzy control.

For this study, a real database was applied for 3 days, from 5 March 2017 to 7 March 2017, at the CRTEn Center: the database included solar radiation, temperature, and humidity. The selected period was characterized by a high variation in wind speed and in global average solar radiation between 0 and 800 W/m^2, due to the position of the greenhouse (very close to the sea).

4.1. Temperature

During the night, the inside temperature was low (7 °C), as is shown in Figure 14. During the same period, the heating system was activated, and the heating rate became more intensive (380 W/m^2)—see Figure 15a—to maintain the inside temperature around its set point of 15 °C (see Figure 14). Meanwhile, the heating rate was at an average level of 120 W/m^2 when the inside temperature was close to the set point. During the day, the ventilation system started operating to remove hot air and to push in cooler outside air; thus, the ventilation rate (Figure 15b) became more intensive (50 m^3/min) in order to reduce the indoor air temperature tp around the set point of 24 °C.

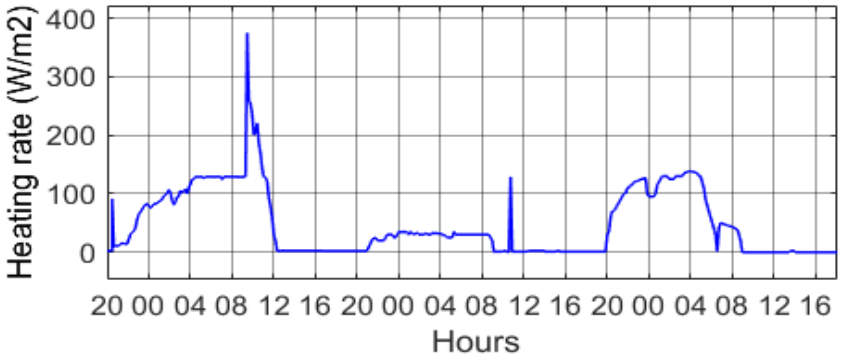

(**a**)

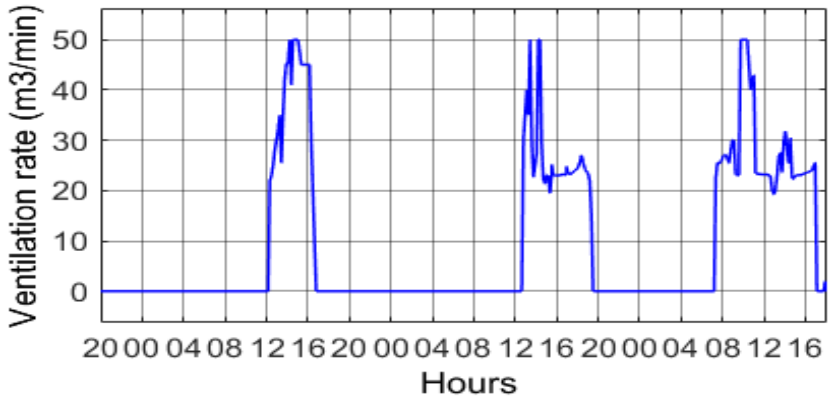

(**b**)

Figure 15. Heating rate (**a**) and ventilation rate (**b**) computed from the fuzzy controller.

4.2. Humidity

The simulation results of the indoor relative humidity (with the control) are reported in Figure 16. The dehumidification system (Figure 17b) was activated with a maximum value of 15 g H_2O/min during the night in order to remove the water vapor accumulated in the indoor climate of the greenhouse. This was needed to maintain the inside humidity around its predefined set point of 80%, but this value could reach more than 97% without the control, as is reported in Figure 6. During the day, the internal humidity was relatively low (Figure 6) without the control due to the effect of the thermal load trapped inside the greenhouse (this reduced the air in the contained water). During this period, the humidification system was activated at a high rate (Figure 17a) to stabilize the humidity level around the set point of 70%.

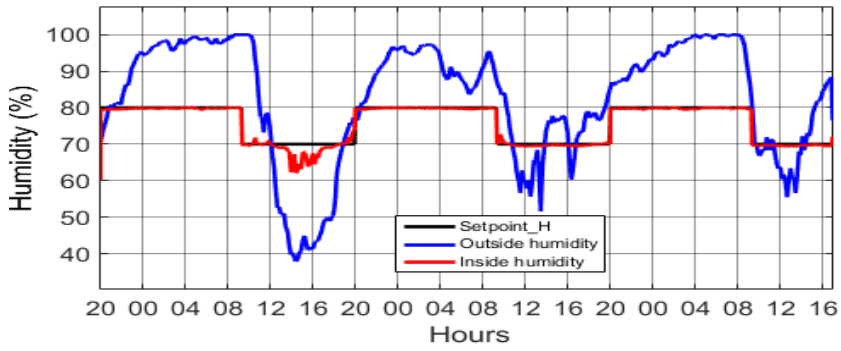

Figure 16. The variation in the relative humidity with the FLC controller.

The simulation results showed the effectiveness of the FLC in controlling the indoor parameters of the agricultural greenhouse. A fuzzy controller was designed to control the inside climate using

appropriate actuators. The results of the simulation showed the efficiency of the developed FLC in meeting the requirements of factories in terms of temperature and humidity and in obtaining a favorable microclimate for the agricultural production of tomato plants.

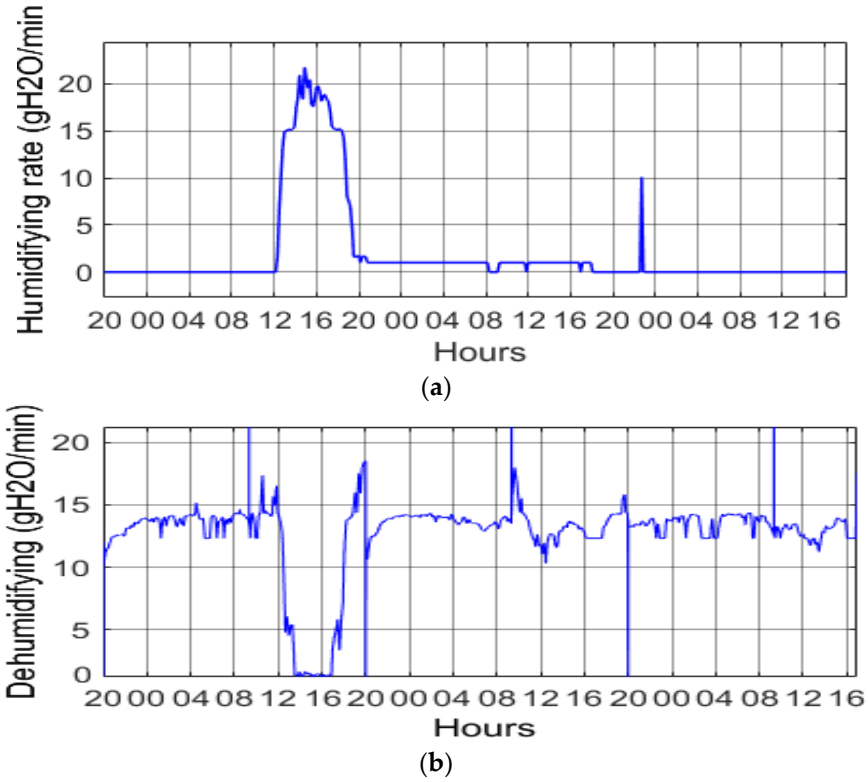

Figure 17. The humidification rate (**a**) and the dehumidification rate (**b**) computed from the fuzzy controller.

5. Photovoltaic System

5.1. Energy Management Approach

In this part, we present the main contribution of this work, which is represented by the coupling of photovoltaic energy in the agricultural sector and by efficiency in the control of the parameters of the agricultural greenhouse.

An agricultural greenhouse requires a lot of energy over the production period in order to promote optimal control of the inside climate.

During the day, the temperature of the environment frequently reaches a high value, so the inside air temperature of the agricultural greenhouse exceeds the predefined set point. Since there is no internal relative humidity, Figures 15b and 17a show the need for ventilation and humidification during the day, when solar radiation reaches a high value. The presence of photovoltaic energy provides an alternative use to avoid burdening the electrical grid; moreover, a solar-powered ventilation system based on a variable speed fan can be adopted using a vector control optimized by fuzzy logic to manage the ventilation flow rate in order to obtain robust control.

5.2. System Description

The PV-based ventilation system (Figure 18) is constituted by the following:

- A PV generator, whose maximum power is assured by the maximum power point tracking MPPT command based on the perturb and observe (P&O) method;

- A power stage consisting of a continuous-to-continuous converter, called single ended primary inductor converter "SEPIC", and an inverter (red block);
- An asynchronous motor that drives the fan; and
- A vector control optimized by fuzzy logic for asynchronous motor speed control (yellow block).

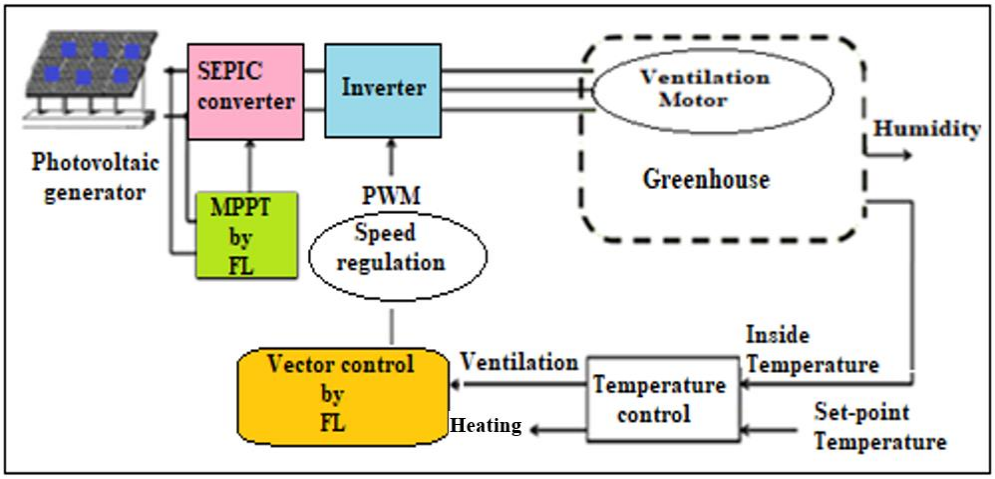

Figure 18. Photovoltaic (PV)-based ventilation system.

5.2.1. Parameters of the PV Modules

The PV generator consists of four series-connected modules. Some parameters of the datasheet of the PV module are shown in Table 3 under standard test conditions (STCs) [30].

Table 3. Parameters of the KANEKA 60.

Electrical Data	Value
Nominal output *Pmpp* (W)	60
Nominal voltage *Vmpp* (V)	67
Nominal current *Impp* (A)	0.9
Open-circuit voltage *Voc* (V)	92
Short-circuit current *Isc* (A)	1.19

The current–voltage (I-V) and power–voltage (P-V) curves of Figure 19 describe the behavior of the PV generator under the STCs (G = 1000 W/m^2 and the ambient temperature T = 25 °C).

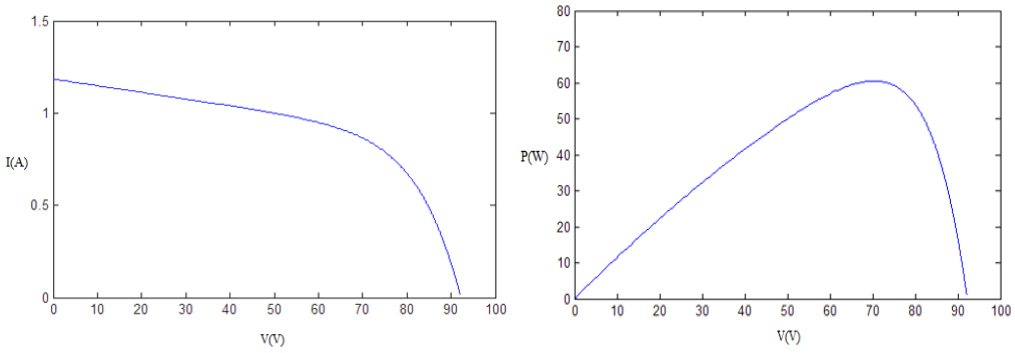

Figure 19. I–V and P–V curves of the KANEKA 60.

The selection of the maximum power point by the optimized P&O algorithm was studied in a work that showed the simulation of the control system based on fuzzy logic techniques (Figure 20).

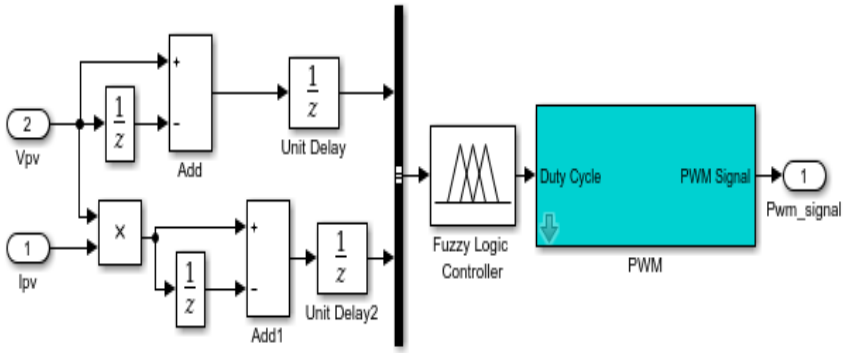

Figure 20. Simulink model of the perturb and observe (P&O)-optimized fuzzy logic strategy (Figure 18, green).

5.2.2. SEPIC Converter

The SEPIC converter chosen for this application is similar to a buck–boost converter, but it has the advantage of noninverted output. SEPIC essentially consists of three capacitors (Cin, Cout, and Cp), two coupled inductors (L1 and L2), a diode (D1), and a transistor (Q1). The output voltage pins are highlighted in red in Figure 21.

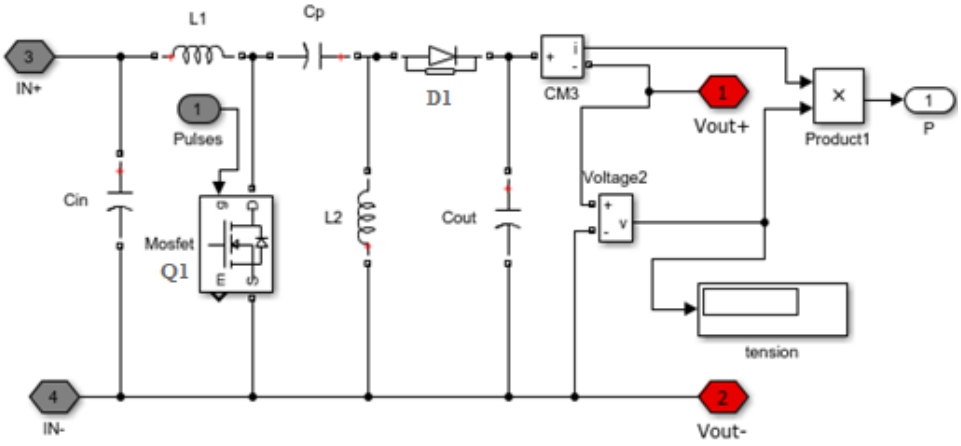

Figure 21. Simulink model of the SEPIC converter.

In the proposed test lab greenhouse, the converter model DV51-322-2K2 is used, with the following values of the components:

- $C_{in} = C_{out} = 440$ µF;
- $C_p = 10$ µF; and
- $L_1 = L_2 = 47$ µF.

Moreover, the efficiency varies from 0.78 to 0.91, with the maximum value being valid for nominal conditions.

5.2.3. DC/AC Inverter

Asynchronous machine speed control systematically includes the use of a static power converter to vary the speed of the inverter. By means of a well-tuned sequence of opening and closing the switching cells (using a DC voltage source), the static converter can switch the current in the phases of the machine in order to obtain a perfectly controllable three-phase current system.

The inverter is controlled by a pulse width modulation strategy. Figure 22 shows a schematic diagram of the inverter feeding a three-phase motor, while the technical specifications are reported in Reference [31]. The three arms of the inverter are controlled by the vector $\begin{pmatrix} \rho A & \rho B & \rho C \end{pmatrix}^T$, with

$$\begin{pmatrix} \rho A \\ \rho B \\ \rho C \end{pmatrix} = \begin{pmatrix} 2 & -1 & -1 \\ -1 & 2 & -1 \\ -1 & -1 & 2 \end{pmatrix} \begin{pmatrix} Pwm1 \\ Pwm2 \\ Pwm3 \end{pmatrix}, \quad (15)$$

where *Pwm*1, 2, and 3 represent the control signals' pulse width modulation (*PWM*), which is generated by the command.

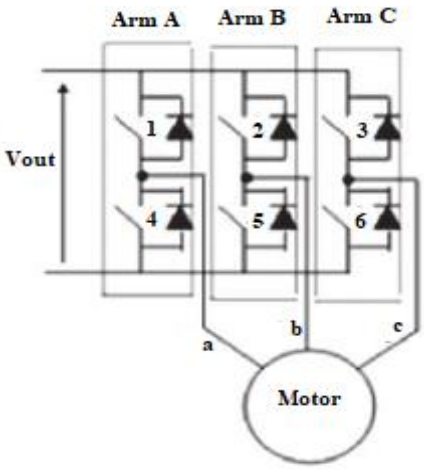

Figure 22. Schematic diagram of the inverter.

5.3. Vector Control Optimized by Fuzzy Logic

A vector command allows for controlling the motor speed, the electromotive flow, and the torque of a three-phase AC electric motor. In general, vector control consists of a PI controller that calculates the speed reference as a function of its nominal speed: this technique is not suitable for the speed regulation of a motor. Therefore, a fuzzy controller provided by a variable speed fan was developed to regulate the reference: this control strategy gave robustness to the proposed command. The calculation of the reference speed (using fuzzy logic based on measurements) is done based on the ventilation rate of the agricultural greenhouse (due to outdoor climate conditions). The ventilation rate depends on the fan speed, so the desired speed is the input of the vector control. The fan speed is calculated by the linear fan law described by the equation [32]

$$V = k \cdot w, \quad (16)$$

where k is a constant and V and w are the required air flow rate (m^3/min) and the motor speed in RPMs, respectively. In the hot season, the temperature exceeds the predefined set point; thus, the ventilation system operates at a maximum speed to refresh the indoor climate and to lower the temperature around its set point. When this on–off sequence is iterated several times to regulate the temperature, the energy consumption is high. The main advantage of this technique is its easy control algorithm, because only the stator current and voltage are measured in estimating the torque and flux [31]. This control strategy allows for a reduction in energy consumption. For the ventilation system, the use of this control is justified in view of its electrical performance, robustness, and simplicity. The structure of the vector control implemented in the proposed model is represented in Figure 23.

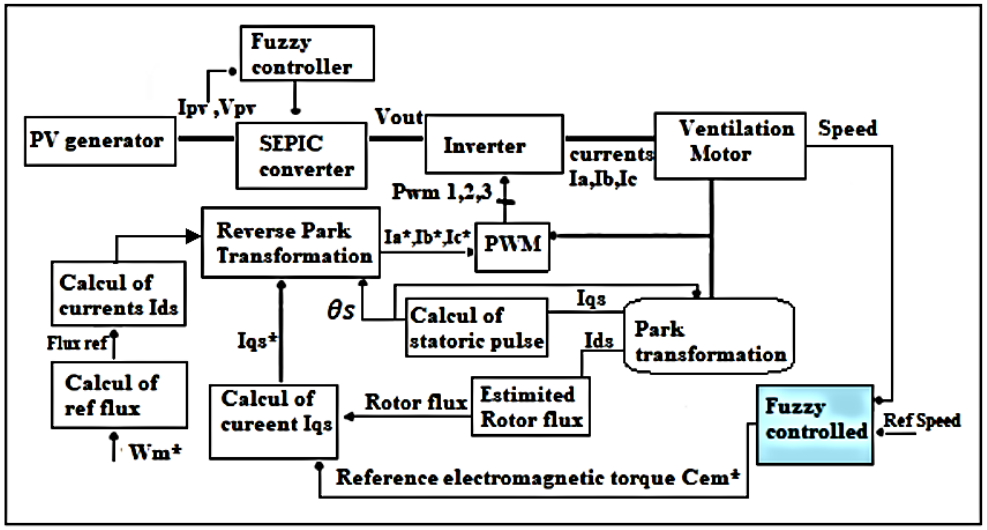

Figure 23. Structure of the optimized vector control using fuzzy logic.

Figure 24 describes the fuzzy controller (the blue block in Figure 23) that determines the electromagnetic field torque Cem, using the speed measurement and its reference.

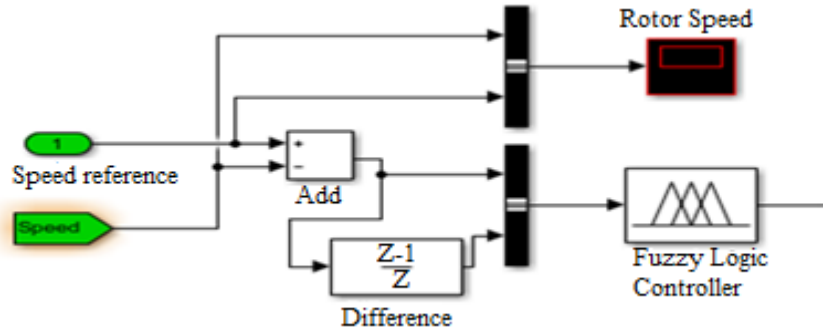

Figure 24. Simulink-based model of the speed controller using fuzzy logic.

5.4. Simulations

The entire system in Figure 23 was simulated in a MATLAB/Simulink environment. The ventilation system was stimulated for a period of two days, with a database of real solar radiation. Motor speed, PV power, and voltage under the control MPPT, solar radiation, and ventilation rate are shown in Figure 25.

The simulation results showed that the control strategy's efficiency and robustness were developed such that during the day, the solar radiation was relatively high (see Figure 25e), and a constant voltage of 260 V (see Figure 25a) (provided by the photovoltaic generator) confirmed the efficiency of the fuzzy MPPT control. This voltage guaranteed a power value of 800 W (Figure 25b) in powering the asynchronous motor that drives the fan at a variable speed. The inside temperature for periods during the day exceeded the reference point, and a high ventilation flow rate of 50 m^3/min (see Figure 25c) was necessary to cool the indoor climate. On the other hand, the active fan had a maximum speed of 480 RPM, as shown in Figure 25d, which was controlled by the fuzzy vector control and lowered the heat accumulation in the indoor climate.

The results obtained showed the speed and performance of the speed control system in different periods and the usefulness of the developed fuzzy controller in meeting the speed instructions.

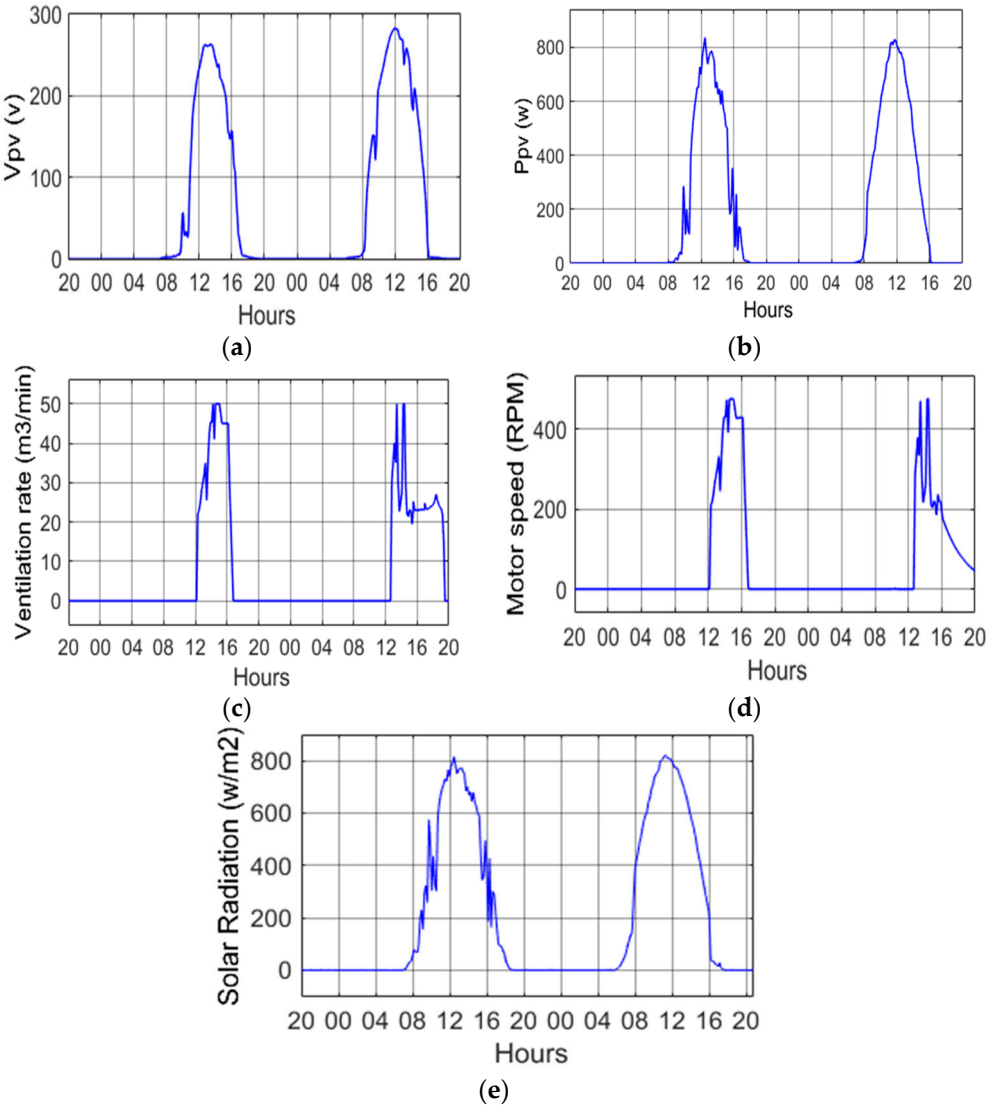

Figure 25. Simulation of the ventilation system powered by the PV system. (**a**) Voltage; (**b**) power; (**c**) ventilation rate; (**d**) motor speed; (**e**) real solar radiation.

6. Conclusions

This paper presents a control system for an agricultural greenhouse powered by a PV system. The dynamic model was presented and experimentally validated. The simulations showed an agreement between the calculated data and the measured data. A fuzzy controller was developed for the smart control of the indoor temperature and humidity, which increases the indoor air temperature overnight to 15 °C and decreases the temperature during the day to 24 °C, keeping a constant value of relative humidity of 70% during the day and 80% during the night. The electrical feeding of the asynchronous motor that drives the variable speed fan is guaranteed by a PV system, with the aim of significantly reducing the use of grid utilities, which results in lower agricultural costs. The power delivered by the photovoltaic generator is 800 W, which is sufficient for the operation of the engine during the day, because the engine absorbs 700 W. A fuzzy vector control was designed for the purpose of controlling the ventilation speed. The simulation results showed the efficiency and the robustness of the fuzzy controller, which guarantees a maximum ventilation speed of 450 RPM.

Although the proposed model was applied to the cultivation of a specific plant (tomato plants) (fixed thresholds of temperature and humidity), it can also be easily extended to other typologies of cultivation. In fact, the values of the geometric and physical parameters of the greenhouse, the

threshold values of temperature and humidity, the power of both electrical loads and the PV plant, and the constraints of the FLC can be modified to extend the use of the proposed model to any greenhouse with other characteristics and other cultivations. Thus, in our opinion, the proposed model can be useful both for greenhouse designers—during the first design stage—and for researchers who focus on greenhouse R&D. Indeed, it is worth noting that greenhouses are increasingly taking on a crucial role in circular economies and in sustainable social and economic development.

Author Contributions: Conceptualization, A.M.; Formal analysis, S.V.; Investigation, J.R.; Methodology, D.M.; Supervision, S.V.; Writing–riginal draft, J.R. and S.V. All authors have read and agreed to the published version of the manuscript.

Funding: This research received no external funding.

Conflicts of Interest: The authors declare no conflict of interest.

Nomenclature

A	Surface of the greenhouse
Ca	Specific heat of air
Ce	Transfer coefficient of water vapor in the air
Ct	Thermal conductivity of the wooden plate
V	Volume
Vr	Ventilation rate
Hr	Heating rate
HuR	Humidification rate
DHuR	Dehumidification rate
C	Cover
ca	Canopy
h_0	Outside convection
V_w	Wind speed
Nh	Number of heaters
Rh	Capacity of heating
Pa	Vapor pressure
U	Overall heat transfer
S	Soil
Tsky	Sky temperature
Inf	Infiltration
Greek symbols	
α	Absorptivity of solar radiations
ρ	Reflectivity
τ	Transmissivity
Subscripts	
RPM	Revolution per minute
GPV	Photovoltaic generator
Ppv	PV power
Vpv	PV voltage
FL	Fuzzy Logic
MPPT	Maximum power-point tracking
P&O	Perturb and observe
Tin	Temperature inside greenhouse
Tout	Temperature outside greenhouse
Dehum	Dehumidifying
Hum	Humidifying
CRTEn	Research and Technology Center of Energy in Borj Cedria, Tunisia

References

1. Hahn, F. Fuzzy controller decreases tomato cracking in greenhouses. *Comput. Elect. Agric.* **2011**, *77*, 21–27. [CrossRef]
2. Ben Ali, R.; Aridhi, E.; Mami, A. Fuzzy Logic Controller of temperature and humidity inside an agricultural greenhouse. In Proceedings of the 2016 7th International Renewable Energy Congress (IREC), Hammamet, Tunisia, 22–24 March 2016.
3. Udinkten Cate, A.J. Modeling and (Adaptive) Control of Greenhouse Climates. Ph.D. Thesis, Agricultural University of Wageningen, Wageningen, The Netherlands, 1983.
4. Liu, X.W.; Dai, T.F. Design for Fuzzy Decoupling Control System of Temperature and Humidity. In *International Conference on Computer Science and Information Engineering*; Springer: Berlin/Heidelberg, Germany, 2011; pp. 231–236.
5. Fourati, F. Multiple neural control of a greenhouse. *Neurocomputing* **2014**, *139*, 138–144. [CrossRef]
6. Taki, M.; Ajabshirchi, Y.; Ranjbar, S.F.; Rohani, A.; Matloobi, M. Heat transfer and MLP neural network models to predict inside environment variables and energy lost in a semi-solar greenhouse. *Energy Build.* **2016**, *110*, 314–329. [CrossRef]
7. Hasni, A.; Taibi, R.; Draoui, B.; Boulard, T. Optimization of greenhouse climate model parameters using particle swarm optimization and genetic algorithms. *Energy Procedia* **2011**, *6*, 371–380. [CrossRef]
8. Ji, R.; Qi, L.; Huo, Z. Design of Fuzzy Control Algorithm for Precious Irrigation System in Greenhouse. *Nonlinear Model Predict. Control* **2012**, *370*, 278–283.
9. Lafont, F.; Balmat, J.F. Optimezd Fuzzy Control of a greenhouse. *Fuzzy Sets Syst.* **2002**, *128*, 47–59. [CrossRef]
10. Atia, D.M.; El-madany, H.T. Analysis and design of greenhouse temperature control using adaptive neuro-fuzzy inference system. *J. Electr. Syst. Inf. Technol.* **2016**, *4*, 34–48. [CrossRef]
11. Mohamed, S.; Hameed, I.A. A GA-based adaptive neuro-fuzzy controller for greenhouse climate control system. *Alex. Eng. J.* **2016**, *57*, 773–779. [CrossRef]
12. Revathi, S.; Sivaku Maran, N. Fuzzy based temperature control of greenhouse. *IFAC PapersOnLine* **2016**, *49*, 549–554. [CrossRef]
13. Azaza, M.; Echaieb, K.; Tadeo, F.; Fabrizio, E.; Iqbal, A.; Mami, A. Fuzzy Decoupling Control of Greenhouse Climate. *Arab. J. Sci. Eng.* **2015**, *40*, 2805–2812. [CrossRef]
14. Dayan, J.; Dayan, E.; Strassberg, Y.; Presnov, E. Simulation and control of ventilation rates in greenhouses. *Math. Comput. Simul.* **2004**, *65*, 3–17. [CrossRef]
15. Villarreal-Guerrero, F.; Kacira, M.; Fitz-Rodrıguez, E. Simulated performance of a greenhouse cooling control strategy with natural ventilation and fog cooling. *Biosyst. Eng.* **2012**, *111*, 217–228. [CrossRef]
16. Boulard, T.; Draoui, B. Natural ventilation of a greenhouse with continuous roof vents: Measurements and data analysis. *J. Agric. Eng. Res.* **1995**, *61*, 27–36. [CrossRef]
17. Esen, M.; Yuksel, T. Experimental evaluation of using various renewable energy sources for heating a greenhouse. *Energy Build.* **2013**, *6*, 340–351. [CrossRef]
18. Abdel-Ghany, A.M.; Kozai, T. Dynamic modeling of the environment in a naturally ventilated, fog-cooled greenhouse. *Renew. Energy* **2006**, *31*, 1521–1539. [CrossRef]
19. Fabrizio, E. Energy reduction measures in agricultural greenhouses heating: Envelope, systems and solar energy collection. *Energy Build.* **2012**, *53*, 57–63. [CrossRef]
20. Azaza, M. Optimized Micro-Climate Controller of a Greenhouse Powered by Photovoltaic Generator. In Proceedings of the 2014 5th International Renewable Energy Congress (IREC), Hammamet, Tunisia, 25–27 March 2014.
21. Echaieb, K.; Azaza, M.; Mami, A. A new control strategy of indoor air temperature in a photovoltaic greenhouse. *Int. J. Soft Comput. Softw. Eng.* **2013**, *3*, 848–852.
22. Vergura, S.; Massi Pavan, A. On the photovoltaic explicit empirical model: Operations along the current-voltage curve. In Proceedings of the IEEE-ICCEP 2015 International Conference on Clean Electrical Power, Taormina, Italy, 16–18 June 2015.
23. Massi Pavan, A.; Vergura, S.; Mellit, A.; Lughi, V. Explicit empirical model for photovoltaic devices. Experimental validation. *Sol. Energy* **2017**, *155*, 647–653. [CrossRef]
24. Acciani, G.; Falcone, O.; Vergura, S. Analysis of the thermal heating of poly-Si and a-Si photovoltaic cell by means of FEM. *Renew. Energy Power Qual. J.* **2010**, 8. [CrossRef]

25. Vergura, S.; Marino, F. Quantitative and Computer Aided Thermography-based Diagnostics for PV Devices: Part I—Framework. *IEEE J. Photovolt.* **2017**, *7*, 822–827. [CrossRef]
26. Vergura, S.; Colaprico, M.; de Ruvo, M.F.; Marino, F. A Quantitative and Computer Aided Thermography-based Diagnostics for PV Devices: Part II—Platform and Results. *IEEE J. Photovolt.* **2017**, *7*, 237–243. [CrossRef]
27. Vergura, S.; Marino, F.; Carpentieri, M. Processing Infrared Image of PV Modules for Defects Classification. In Proceedings of the International Conference on Renewable Energy Research and Applications (ICRERA), Palermo, Italy, 22–25 November 2015.
28. Ben Ali, R.; Bouadila, S.; Mami, A. Development of a Fuzzy Logic Controller applied to an agricultural greenhouse experimentally validated. *Appl. Therm. Eng.* **2018**, *141*, 798–810. [CrossRef]
29. Echaieb, K.; Marouani, R.; Mami, A. Nonlinear multivariable design control strategy of solar water pumping system. *Eur. J. Sci. Res.* **2012**, *72*, 539–548.
30. Chaouali, H.; Othmani, H.; Mezghani, D.; Jouini, H.; Mami, A. Fuzzy logic control scheme for a 3 phased asynchronous machine fed by Kaneka GSA-60 PV panels. In Proceedings of the 7th IEEE International Conference on Renewable Energy Congress, Hammamet, Tunisia, 22–24 March 2016.
31. Mezghani, D.; Othmani, H.; Mami, A. Bond graph modeling and robust control of a photovoltaic generator that powered an induction motor pump via SEPIC converter. *Int. Trans. Electr. Energy Syst.* **2019**, *29*, e2746. [CrossRef]
32. Azaza, M.; Echaieb, K.; Fabrizio, E.; Iqbal, A.; Mami, A. An intelligent system for the climate control and energy savings in agricultural greenhouses. *Energy Effic.* **2016**, *9*, 1241–1255. [CrossRef]